

UDAC: Under-Display Array Cameras

Chengyu Wang¹ Jing Li¹ Pavan C. Madhusudanarao¹ Jinhan Hu¹ Jitesh K. Singh²
WooJhon Choi³ Seok-Jun Lee¹ Hamid R. Sheikh¹

¹Samsung Research America ²Samsung Research India-Bangalore ³Samsung Electronics

{chengyu.wang, jing.li1, pavan.m1, jh.hu1, jitesh.kr,
woojhon.choi, seokjun1.lee, hr.sheikh}@samsung.com

Abstract

Under-display cameras (UDC) provide uninterrupted display experience on smartphones, but the captured images suffer from quality degradations such as diffraction blur, and reduced signal-to-noise ratio due to the presence of the OLED panel which obstructs the camera. In this work, we propose to use under-display array cameras (UDAC) consisting of two cameras placed under the OLED display panel to further reduce image artifacts and enhance image quality. We rotate the OLED panel by 45 degrees for one of the cameras to utilize the complimentary nature of the point spread function. We also propose an algorithm to combine images from the two cameras, which includes occlusion and optical flow analysis, image warping, color match and image blending. Experiments on real UDC devices show that the proposed method is superior in reducing the artifacts and improving the signal-to-noise ratio. The proposed method is simple but effective, and it can be easily extended to various configurations and incorporated with various algorithms.

1. Introduction

Under-display Cameras (UDC) in smartphones provide uninterrupted display experience for large screen devices by eliminating the need for a “punch hole” in the display through which a camera can take pictures. As shown in Fig. 1, the camera assembly (lens and sensor) of an UDC is placed behind a specialized display panel that allows some light to pass through transparent inter-pixel gaps in the display. Compared with a punch-hole camera, an UDC achieves large screen-to-body ratio and improves user experience, but the image quality of an UDC is substantially reduced because the OLED pixels reduce the light that reaches the sensor. The lower light transmission rate results in poor signal-to-noise ratio, and the display panel produces various optical artifacts, such as diffraction [13] and scatter effect [17], which result in blurry and hazy images. One

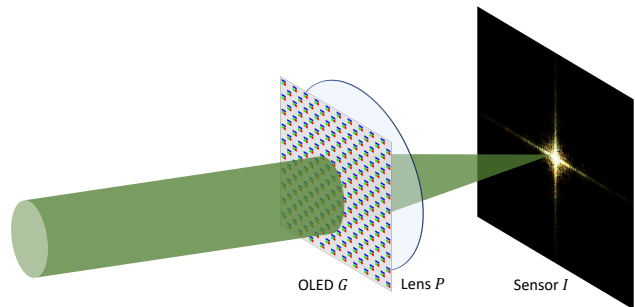


Figure 1. The layout of an under-display camera. The camera sensor is placed under the transparent display panel, and the partial pass OLED pattern results in degradation of the point spread function.

method to alleviate these artifacts is to increase the transparent area on the panel and improve the design of the OLED layout to reduce the diffraction artifacts [20], but this affects the invisibility of the camera and reduces the quality of the display. Sophisticated image restoration techniques are therefore critical for UDC systems.

Various neural network based methods have been proposed in recent years to solve the UDC image degradation issue [6, 7, 12, 13, 17, 22]. In these methods, paired training data are usually obtained via a monitor camera imaging system (MCIS) or from simulations using point spread function (PSF) modeled from a binary display mask. However, there are several disadvantages associated with these methods. In an MCIS setup, an OLED display panel is placed in front of a traditional camera to imitate an UDC, but such a system has different optical features from a real UDC device. Similarly, using a simulated PSF can also be problematic in the simulation scenario. Firstly, optical modeling of the PSF can be inaccurate because the OLED panel is simply modeled as a binary mask. Secondly, a single PSF is not enough to describe the imaging process. In fact, it has been observed that the change in the angle of incidence results in distorted PSF, i.e., shift-variant PSF [13]. Third, mea-

asuring a PSF using an UDC device requires the access to the unprocessed raw data and knowledge of the physical characteristics of the imaging sensor. Although the aforementioned methods resolve some of these issues, it is still difficult to address all of them to obtain the accurate data for network training. Besides, all these methods focus on the image restoration for a single UDC image without considering the system level innovation.

Inspired by the success of array cameras in computational imaging [1], particularly for diffraction removal [19], here we consider further improving the image quality using multiple UDCs, named as under-display array cameras (UDAC). While we specifically describe a two-camera array, the proposed techniques described in this paper can be generalized to more than two cameras in the array. As shown in Fig. 2a, the PSF of an UDC exhibits spikes because of the presence of wires and OLED pixels. By using two cameras with the rotated OLED pattern and a suitable blending algorithm to combine the two images, we can reduce the diffraction artifacts and improve the signal-to-noise ratio. We also consider the 3D occlusion due to the different camera viewpoints and the color difference between two images so that the proposed method can be easily adapted to different configurations. The major contributions of this paper can be summarized as follows:

- We propose a new system for under-display imaging based on optical analysis that is composed of two UDCs, and the OLED display patterns of the two cameras are related with a rotation transformation.
- We provide a modularized imaging algorithm which contains optical flow estimation, occlusion mask generation, color match, image warping and blending.
- Experiments with a commercial UDC device are conducted to show significant image quality improvement of the proposed approach compared to a single UDC.

2. Related Work

2.1. UDC Restoration

UDC image restoration has been an emerging topic of interest among the imaging community since early 2020s. The earlier works were pioneered by Zhou *et al.* [22] and the UDC 2020 Challenge [21], and many deep learning based methods have been proposed thereafter. UDC images are affected by a multitude of quality degradations, and the most studied degradations are the diffraction blur and the increased noise due to the presence of partial pass OLED panel. Oh *et al.* [15] used a modified U-net with dilated convolutions and residual connections for UDC image restoration. Conde *et al.* [3] developed a light U-net based network that achieved real-time computation on smartphone GPUs. Feng *et al.* [6] proposed a dynamic skip connection network to inverse the diffraction blur given the PSF of the sys-

tem. Kwon *et al.* [13] built a controllable network that utilized the per-pixel kernel representation to address the shift variant blur. Kim *et al.* [11] proposed joint demosaicking and deblurring for the Quad Bayer color filter array which is commonly used in modern smartphone cameras. Qi *et al.* [16] proposed a RAW-to-RAW pipeline that worked with any image processing pipelines. Zhou *et al.* [23] employed generative adversarial network framework for both simulating and restoring the UDC image.

The display panel in front of the camera also affects the spectrum of the incident light and the light permeation, which results in reduced contrast and saturation. Luo *et al.* [14] analyzed the data distribution in the hue, saturation and value channels of UDC images and proposed a semi-supervised approach to enhance the images. Koh *et al.* [12] boiled down the degradations in UDC images to the diffraction blur and the color filtering operation and proposed a two-branched method to restore the image. Similarly Gao *et al.* [8] proposed a two-stage restoration method that restored the color and the detail sequentially given two differently exposed UDC images. Song *et al.* [17] analyzed the haziness and contrast distortion caused by the UDC scattering effect and proposed to utilize a scattering branching in image restoration.

2.2. UDC Dataset

The primary challenge in training an UDC restoration network is acquiring paired training data. The first UDC dataset was created by Zhou *et al.* [22], where the paired dataset was obtained from a MCIS setup. A 4K LCD monitor was used to display natural images, and a T-OLED or P-OLED panel was installed in front of an RGB camera to capture the images. This setup was further enhanced by Qi *et al.* [16] that explored the usage of HDR monitor data. Although these work provided the dataset for UDC Restoration research and inspired the development of new algorithms [3, 15, 18, 23], the data captured by a MCIS setup suffered from the low dynamic range of the monitor and could not match the real world scenes, especially bright outdoor scenes. More recently synthetic data has been used in the experiments, which requires the acquisition of the PSF of the imaging system. Kwon *et al.* [13] considered the angle of incident of the incoming light and modeled the shift variant PSF using the orthogonal projection of the OLED panel. Although optical modeling provides the theoretical PSF of an optical system, it still differs from the PSF of a real UDC system due to the approximated system parameters and manufacturing imperfections. In [6] and [8] the PSF captured by an UDC setup was employed to generate a synthetic dataset to remedy this issue. However, models trained on synthetic data with estimated PSF have limited generalization across real-world scenarios because of the proximity of the complicated degradation. Re-

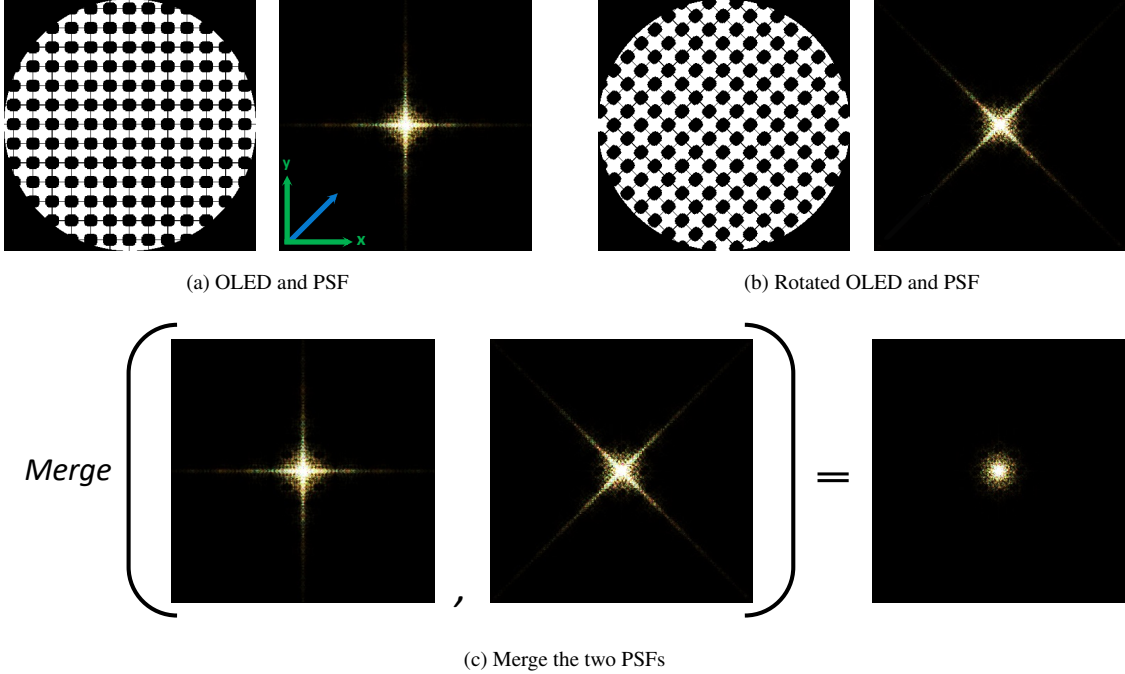


Figure 2. PSF analysis of UDC and UDAC. The PSF pattern of the camera rotates with the OLED pattern, and combining the rotated PSF by retaining the minimum value yields a more concentrated PSF.

cently, Feng *et al.* [7] proposed a Transformer based method to align misaligned data for generating high-quality paired data.

3. Under-display Array Cameras

The degradation of the UDC image quality comes from various aspects. Here we focus on the effect of light diffraction. Fig. 1 illustrates the layout of an UDC system. An OLED display with pattern G is placed on top of the camera lens with the aperture P . According to the Fourier Optics [9], a Fraunhofer diffraction pattern corresponding to the field in front of lens is observed at the focal plane behind the lens. The PSF intensity at the focal plane can be written as

$$h = |\mathcal{F}(GP)|^2, \quad (1)$$

where \mathcal{F} represents the Fourier transform. Note that in Eq. (1) constant terms and scaling factors are ignored for simplicity. We consider a binary OLED pattern and the corresponding PSF shown in Fig. 2a. Because of the wires and LEDs on the panel, the binary aperture contains straight edges which results in spikes in the PSF and therefore orientation dependent imaging performance in an UDC system. This can be characterized by the orientational MTFs illustrated in Fig. 3, where the MTFs along two directions, denoted by the green (axial) and the blue (diagonal) arrows in Fig. 2a are simulated. While diagonal MTF has higher value for high frequency signals, axial MTF has higher value for

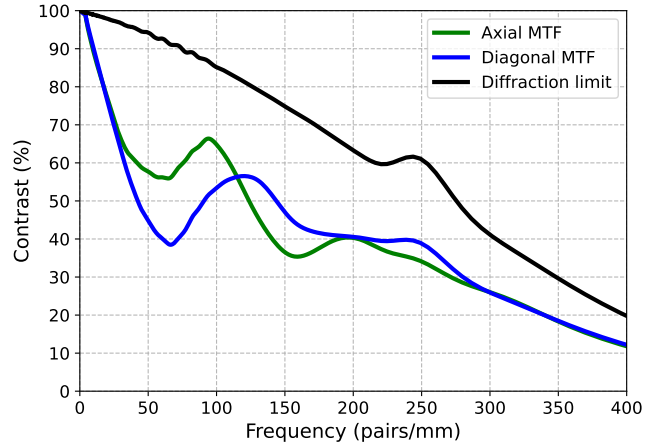


Figure 3. MTF analysis of UDC. The simulated MTFs for axial direction (green), diagonal direction (blue) and OLED-free camera (black) are shown. In an UDAC system, the system MTF can be maximized by combing the MTFs of the two orientations: $\max(\text{MTF}_1(\nu), \text{MTF}_2(\nu))$.

low frequency signals.

Inspired by the nature of the PSF of an UDC system, we propose a multi-camera system titled under-display array cameras (UDAC) with the main goal of reducing diffraction artifacts and significantly improving image quality. To utilize the complimentary nature of the PSF, **the OLED patterns of the two cameras are not identical but related**



Figure 4. The performance of the proposed method on 2D scenes. The effectiveness of UDAC in diffraction removal can be observed around the light source and the railings.

by a 45-degree rotation transformation. As illustrated in Fig. 2b, the spikes in the PSF rotates with the OLED pattern. If the two PSFs are combined to retain the smaller value for each pixel, the spikes can be removed (see Fig. 2c).

The advantage of the pattern rotation can also be seen from the MTF of the system. With the pattern rotation, the blending algorithm essentially combines the two images with different MTFs. In this paper, we use a simple algorithm to blend the images based on spatial frequency, and obtain the maximum value for each frequency:

$$MTF_{blend}(\nu) = \max(MTF_1(\nu), MTF_2(\nu)). \quad (2)$$

As a proof of concept, we created a 2D scene with a printed poster image and added a light source using a LED button lamp. A 2D scene is selected to avoid artifacts from inaccurate 3D registration. Sec. 5 provides more details on the capture setup. In Fig. 4 we compare the blended image using the proposed UDAC system with a single UDC image produced using the built-in image signal processing pipeline which contains a PSF inversion module to restore the image from the diffraction blur. We also include the result when this built-in PSF inversion module is disabled. While the restoration for a single image can improve the resolution and reduce the diffraction artifacts, it is clear that UDAC can further reduce artifacts significantly.

Developing unique OLED patterns with the aim of reducing diffraction can be challenging as the invisibility of the UDC is a paramount design consideration. A UDAC system with rotated OLED patterns provides an easy and effective solution to address diffraction artifacts seen in UDC systems.

It is worth-noting that the proposed rotation of the OLED pattern can be achieved in various methods. For example, other than using two cameras with rotated OLED pattern, one can use mechanically rotatable OLED or manually rotate the device. Both of these methods require two captures using a single camera.

4. Method

Improving image quality with under-display array cameras is not trivial. Merging two images captured from different viewpoints requires finding the pixel correspondence between them. To achieve that, the extrinsic parameters of the cameras, lens aberration and occlusion in the 3D scenes need to be addressed, and the auto exposure/ISO/white-balance in the smartphone cameras need to be compensated. To this end, we present a data processing method for a UDAC system that can improve UDC image quality effectively, as shown in Fig. 5. Our method contains several modules including global warping, scene analysis with optical flow and occlusion estimation, local optical flow warping, color match, occlusion substitution and image blending.

We denote the two input images I_1 and I_2 , and the output image I_{out} shares the same viewpoint as I_1 . Firstly, the camera translation and rotation are addressed with **global warping** where the homography transformation is estimated and I_2 is warped as I_2^{global} , to match I_1 . Next, the lens aberration, 3D occlusion and the inaccurate global warping are addressed with the **optical flow** and the **occlusion map** analysis, after which the analysis result is used

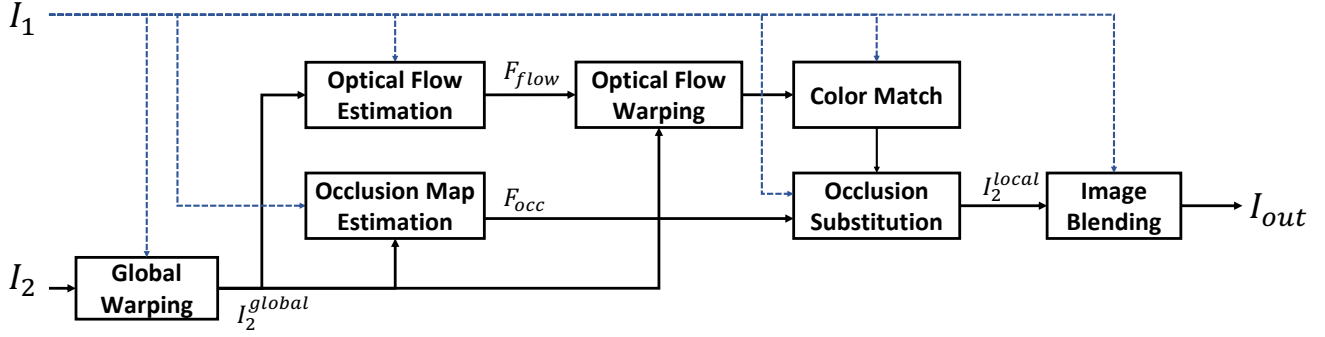


Figure 5. An overview of the UDAC processing pipeline. **Global warping** is first used to compensate the global motion, and the two images are more accurately aligned with **optical flow estimation**, **occlusion map estimation** and **optical flow warping**. **Color match** and **occlusion substitution** are then executed before the UDAC output is generated from **image blending**.

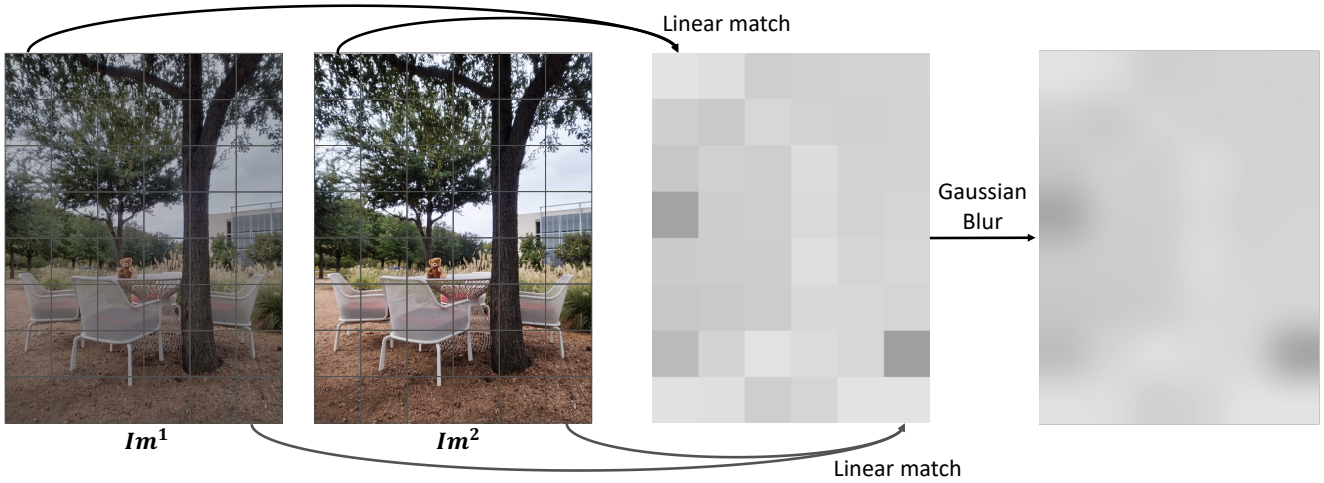


Figure 6. Illustration of the proposed color match method. The images are divided into patches and the linear match is applied to each patch individually. A Gaussian blur is applied afterwards to ensure smooth transition between patches.

to perform **local warping**. The optical flow, F_{flow} , shows the pixel level correspondence between the two images, whereas the occlusion map, F_{occ} , estimates the pixels that appears in I_1 but not in I_2^{global} , such that the occluded pixels in those regions in I_2^{global} will be substituted by pixels in I_1 before two images are blended.

However, there exists brightness/tone difference between the two images due to the aforementioned camera settings. Thus, direct blending of the two images results in artifacts. This issue can be addressed with global linear match, i.e., finding a global linear transformation $\{\alpha, \beta\}$:

$$\alpha^*, \beta^* = \arg \min_{\alpha, \beta} \sum_{n=1}^N (I_2^n * \alpha + \beta - I_1^n), \quad (3)$$

where N represents the number of pixels in each image. However, as we show in the next section, the global linear match is often inadequate and the brightness/color tones

still differ locally. To address this we propose a local linear **color match** method, as shown in Fig. 6. In this method, the images are divided into patches and the linear transform coefficients for each patch is calculated. To avoid boundary artifacts, a Gaussian blur is applied to the coefficient maps before applying the linear transform. The local warp and the color match can be summarized by

$$I_2^{local} = Match(Warp(I_2^{global}, F_{flow}) | I_1) * F_{occ} + I_1 * (1 - F_{occ}), \quad (4)$$

where $Warp$ represents the local warp guided by optical flow, $Match(\cdot | I_1)$ represents color match with reference I_1 . The two registered images I_1 and I_2^{local} are finally **blended** to produce the output image I_{out} .

Note that the proposed UDAC system is built on top of the existing single UDC image restoration. While the latter seeks to inverse the PSF to restore the image, the former exploits the complimentary nature of the PSF.

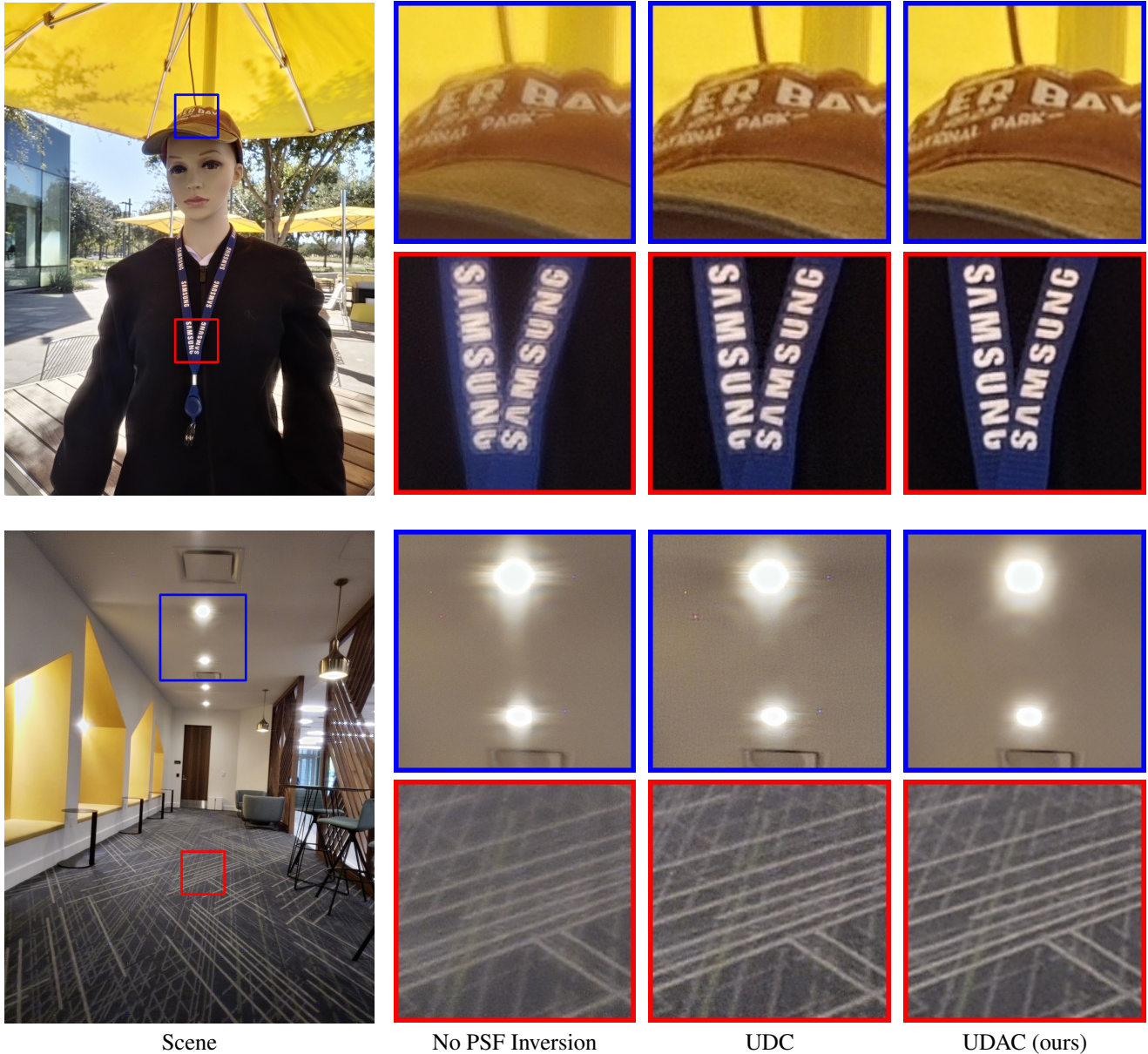


Figure 7. Comparison between a single UDC and the proposed UDAC system.

5. Experiments

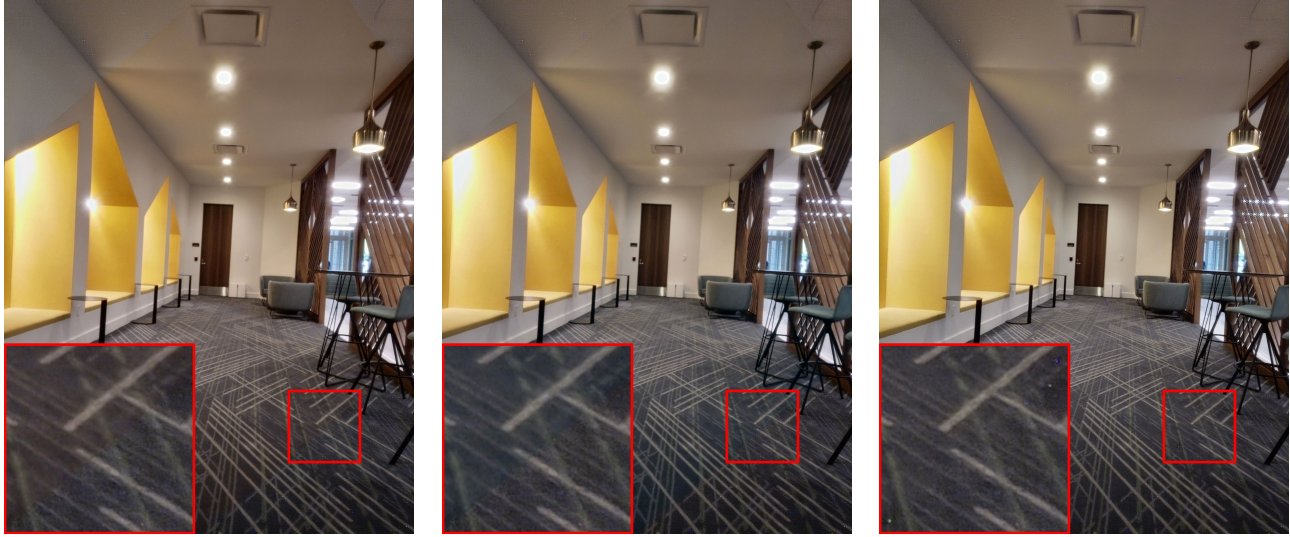
5.1. Implementation Details

We conducted the experiments using a Samsung Galaxy Z Fold 5 with built-in 3A (auto focus, auto exposure and auto white-balance) control. The image resolution is 2304×1728 . The OLED rotation is achieved by rotating the cell-phone by 45 degrees, and we also included the camera translation to introduce different viewpoints. The rotation was compensated by the global warping. For the optical flow and the occlusion map estimation, we used pretrained RAFT [4] and IRR [10] respectively, and for the final merg-

ing we used pyramid blending [2, 5]. In the color match step, the images were divided into 48 patches, each with 288×288 pixels.

5.2. Results

We evaluated the entire pipeline under nature 3D scenes. The results are shown in Fig. 7. The single UDC output with built-in PSF inverse is denoted as “UDC”, and the single UDC output without built-in PSF inverse is denoted as “No PSF Inversion”. Compared with the PSF inversion for a single UDC, the proposed method can further reduce diffraction effect, resulting in more details and less artifacts



(a) No color match

(b) Global method

(c) Proposed method

Figure 8. Comparison between the global linear match and the proposed local linear match method: (a) no color match, (b) the global linear match, and (c) the proposed method.



(a)

(b)

(c)

Figure 9. Examples of failed cases due to (a) inaccurate optical flow, (b) inaccurate occlusion map, or (c) scene dynamics.

in the output image. Reduced noise can also be achieved by blending multiple images.

We then compare the global linear match and the proposed local linear match in Fig. 8. In this example, the two captures had different tones, and the global linear match was able to improve the image color for the ceiling but failed at the carpet. In contrast, the proposed local linear match successfully adjusted the color for all the regions, and no blending artifacts were observed in the output image.

The performance of the proposed method relies on the

accurate optical flow and occlusion estimation. In Fig. 9 we show the failed cases due to inaccurate optical flow, occlusion map or scene dynamics. Note that the networks used in the experiments were pretrained on clear images, while UDC data suffered from high noise and diffraction blur. Training these networks with UDC data can further improve the final output image quality.

6. Conclusion

We presented a multi-camera system for under-display imaging using rotated OLED panel, and we described the image processing pipeline to blend images that consider the occlusion in the scene. We also proposed a color match method to compensate color mismatch arising due to the camera 3A settings. The evaluation with a commercial UDC device showed that the proposed method outperformed image restoration on a single UDC image. As part of future work we plan to incorporate the single UDC restoration into the processing pipeline and achieve joint image restoration, which can reduce the overall computation and produce better results.

References

- [1] David J Brady, Minghao Hu, Chengyu Wang, Xuefei Yan, Lu Fang, Yiwnheng Zhu, Yang Tan, Ming Cheng, and Zhan Ma. Smart cameras. *arXiv:2002.04705*, 2011. [2](#)
- [2] Peter J Burt and Edward H Adelson. A multiresolution spline with application to image mosaics. *ACM Trans. Graph.*, 2(4):217–236, 1983. [6](#)
- [3] Marcos V Conde, Florin Vasluianu, Sabari Nathan, and Radu Timofte. Real-time under-display cameras image restoration and hdr on mobile devices. In *European Conference on Computer Vision*, pages 747–762. Springer, 2022. [2](#)
- [4] MMFlow Contributors. MMFlow: Openmmlab optical flow toolbox and benchmark. <https://github.com/open-mmlab/mmflo>, 2021. [6](#)
- [5] Zeev Farbman, Raanan Fattal, and Dani Lischinski. Convolution pyramids. *TOG*, 30(6):175, 2011. [6](#)
- [6] Ruicheng Feng, Chongyi Li, Huaijin Chen, Shuai Li, Chen Change Loy, and Jinwei Gu. Removing diffraction image artifacts in under-display camera via dynamic skip connection network. In *CVPR*, pages 662–671, 2021. [1](#), [2](#)
- [7] Ruicheng Feng, Chongyi Li, Huaijin Chen, Shuai Li, Jinwei Gu, and Chen Change Loy. Generating aligned pseudo-supervision from non-aligned data for image restoration in under-display camera. In *CVPR*, pages 5013–5022, 2023. [1](#), [3](#)
- [8] KeMing Gao, Meng Chang, Kunjun Jiang, Yaxu Wang, Zhihai Xu, Huajun Feng, Qi Li, Zengxin Hu, and YueTing Chen. Image restoration for real-world under-display imaging. *Optics Express*, 29(23):37820–37834, 2021. [2](#)
- [9] Joseph W Goodman. *Introduction to Fourier optics*. Roberts and Company publishers, 2005. [3](#)
- [10] Junhwa Hur and Stefan Roth. Iterative residual refinement for joint optical flow and occlusion estimation. In *CVPR*, 2019. [6](#)
- [11] Irina Kim, Yunseok Choi, Hayoung Ko, Dongpan Lim, Youngil Seo, Jeongguk Lee, Geunyoung Lee, Eundoo Heo, Seongwook Song, and Sukhwan Lim. Under display camera quad bayer raw image restoration using deep learning. *Electronic Imaging*, 2021(7):67–1, 2021. [2](#)
- [12] Jaihyun Koh, Jangho Lee, and Sungroh Yoon. Bnucd: A two-branched deep neural network for restoring images from under-display cameras. In *CVPR*, pages 1950–1959, 2022. [1](#), [2](#)
- [13] Kinam Kwon, Eunhee Kang, Sangwon Lee, Su-Jin Lee, Hyong-Euk Lee, ByungIn Yoo, and Jae-Joon Han. Controlable image restoration for under-display camera in smartphones. In *CVPR*, pages 2073–2082, 2021. [1](#), [2](#)
- [14] Jun Luo, Wenqi Ren, Tao Wang, Chongyi Li, and Xiaochun Cao. Under-display camera image enhancement via cascaded curve estimation. *IEEE Transactions on Image Processing*, 31:4856–4868, 2022. [2](#)
- [15] Youngjin Oh, Gu Yong Park, Haesoo Chung, Sunwoo Cho, and Nam Ik Cho. Residual dilated u-net with spatially adaptive normalization for the restoration of under display camera images. In *2021 Asia-Pacific Signal and Information Processing Association Annual Summit and Conference (AP-SIPA ASC)*, pages 151–157. IEEE, 2021. [2](#)
- [16] Miao Qi, Yuqi Li, and Wolfgang Heidrich. Isp-agnostic image reconstruction for under-display cameras. *arXiv preprint arXiv:2111.01511*, 2021. [2](#)
- [17] Binbin Song, Xiangyu Chen, Shuning Xu, and Jiantao Zhou. Under-display camera image restoration with scattering effect. In *ICCV*, pages 12580–12589, 2023. [1](#), [2](#)
- [18] Varun Sundar, Sumanth Hegde, Divya Kothandaraman, and Kaushik Mitra. Deep atrous guided filter for image restoration in under display cameras. In *Computer Vision—ECCV 2020 Workshops: Glasgow, UK, August 23–28, 2020, Proceedings, Part V 16*, pages 379–397. Springer, 2020. [2](#)
- [19] Chengyu Wang, Minghao Hu, Yuzuru Takashima, Timothy J Schulz, and David J Brady. Snapshot ptychography on array cameras. *Opt. Express*, 30(2):2585–2598, 2022. [2](#)
- [20] Anqi Yang and Aswin C Sankaranarayanan. Designing display pixel layouts for under-panel cameras. *IEEE Transactions on Pattern Analysis and Machine Intelligence*, 43(7):2245–2256, 2021. [1](#)
- [21] Yuqian Zhou, Michael Kwan, Kyle Tolentino, Neil Emerton, Sehoon Lim, Tim Large, Lijiang Fu, Zhihong Pan, Baopu Li, Qirui Yang, et al. Udc 2020 challenge on image restoration of under-display camera: Methods and results. In *Computer Vision—ECCV 2020 Workshops: Glasgow, UK, August 23–28, 2020, Proceedings, Part V 16*, pages 337–351. Springer, 2020. [2](#)
- [22] Yuqian Zhou, David Ren, Neil Emerton, Sehoon Lim, and Timothy Large. Image restoration for under-display camera. In *CVPR*, pages 9179–9188, 2021. [1](#), [2](#)
- [23] Yang Zhou, Yuda Song, and Xin Du. Modular degradation simulation and restoration for under-display camera. In *Proceedings of the Asian Conference on Computer Vision*, pages 265–282, 2022. [2](#)